AIP | Applied Physics Letters

Strain modulated optical properties in BiFeO3 thin films

H. L. Liu, M. K. Lin, Y. R. Cai, C. K. Tung, and Y. H. Chu

Citation: Applied Physics Letters **103**, 181907 (2013); doi: 10.1063/1.4827639
View online: http://dx.doi.org/10.1063/1.4827639
View Table of Contents: http://scitation.aip.org/content/aip/journal/apl/103/18?ver=pdfcov
Published by the AIP Publishing

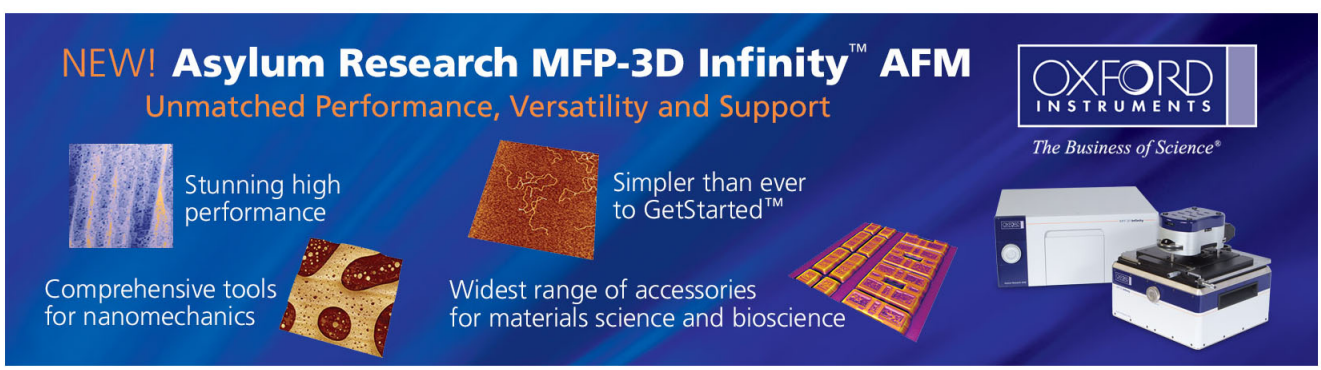

Strain modulated optical properties in $BiFeO_3$ thin films

H. L. Liu,[1,a)] M. K. Lin,[1] Y. R. Cai,[1] C. K. Tung,[2] and Y. H. Chu[2]
[1]*Department of Physics, National Taiwan Normal University, Taipei 11677, Taiwan*
[2]*Department of Material Science and Engineering, National Chiao Tung University, Hsinchu 30010, Taiwan*

(Received 30 August 2013; accepted 16 October 2013; published online 30 October 2013)

Spectroscopic ellipsometry was used to investigate the strain-dependent optical properties of $BiFeO_3$ thin films. At room temperature, the compressively strained $BiFeO_3/LaAlO_3$ thin films show the largest band gap of about 3.12 eV. It redshifts to 2.75 eV for the tensile strained $BiFeO_3/NdScO_3$ thin films. With increasing temperature, observable anomalies in the band gap for all strained thin films near 640 K indicate that antiferromagnetic transition temperature is independent of strain and close to its bulk value, which are in good agreement with the first-principles calculations. These results further suggest a complex nature of charge-spin coupling in multiferroic $BiFeO_3$ thin films. © *2013 AIP Publishing LLC*. [http://dx.doi.org/10.1063/1.4827639]

Multiferroic oxides have recently attracted enormous attention, stimulated not only by their potential usefulness in technological field of the magnetoelectric effect but also for the need to understand the mechanisms underlying their intrinsic coupling between magnetic and electric order parameters.[1–3] Among them, bismuth ferrite, $BiFeO_3$ (BFO), is the most intensively studied multiferroic system[4] because its polar and magnetic orders coexist at room temperature. Below the Curie temperature ($T_C \sim 1100$ K), bulk BFO is described by the rhombohedral $R3c$ space group that allows antiphase octahedral tilting and ionic displacements from the centrosymmetric positions about and along the same [111] pseudocubic direction, respectively. In addition to the G-type antiferromagnetic spin ordering, a cycloid-type spatial spin modulation occurs below the Nèel temperature ($T_N \sim 640$ K). Furthermore, BFO has shown many exotic properties including magnetoelectric coupling, a large remanent polarization, and photovoltaic effect. These advantages make BFO a promising material for the applications in spintronics, multiple-controlled devices, and polar oxide-based solar cells.[5]

There has been particular interest recently in the influence of substrate-induced strain on structure, polarization, and magnetization of BFO thin films.[6] Controlling their physical properties during fabrication is essential for the device applications. The films often have different symmetries and polarizations compared to bulk materials due to lattice mismatch between the film and the substrate. For example, BFO single crystal has a spontaneous polarization value of ~3.5 and ~6.1 $\mu C/cm^2$ along (100) and (111) directions, respectively.[7] In contrast, epitaxial BFO thin films on $SrTiO_3$ substrate show dramatically increased values of remanent polarization (~98 $\mu C/cm^2$) and magnetization (~150 emu/cc).[8,9] More recent theoretical studies predicted that BFO thin films grown on $LaAlO_3$ substrate have a high polarization value of over 150 $\mu C/cm^2$.[10–12]

Up to now, different researchers have reported on the optical properties of BFO thin films.[13–19] In earlier studies, Basu *et al.*[13] reported the first optical transmittance measurements of BFO thin films with 100 nm thick grown on $DyScO_3$ (110) substrates. Room-temperature optical absorption spectra show a direct band gap (2.667 ± 0.005 eV) and two charge transfer excitations at about 3.2 and 4.5 eV. With increasing temperature, the gap softens significantly through both 380 K and T_N. Kumar *et al.*[14] examined the room temperature refractive index and absorption versus wavelength of BFO thin films grown on $SrTiO_3$ (111) substrates using spectroscopic ellipsometry. They found a direct band gap at about 2.81 eV. Ihlefeld *et al.*[15] studied the band gap value of five different molecular-beam epitaxy (MBE)-grown BFO thin films on (001) $SrTiO_3$ (001), (001) $(LaAlO_3)_{0.3}$-$(SrAl_{0.5}Ta_{0.5}O_3)_{0.7}$ (LSAT), and (111) $SrTiO_3$. In all cases, BFO thin films reveal a direct band gap at about 2.77 ± 0.04 eV. The invariance of the band gap energy with films of differing strain states suggests that the band gap is relatively insensitive to these effects. This value is consistent with theoretical predictions using the screened exchange method.[16] Recently, Chen *et al.*[17] employed both optical transmission spectroscopy and spectroscopic ellipsometry to extract the optical properties of quasi-tetragonal BFO thin films with thicknesses between 23 and 38 nm deposited on $YAlO_3$ (110) substrates. The room-temperature absorption spectrum is overall blue shifted compared with that of rhombohedral BFO, with a direct 3.1 eV band gap, and charge transfer excitations that are 0.4 eV higher than those of the rhombohedral counterpart. Allibe *et al.*[18] presented the results of optical transmittance measurements of 400–900 nm epitaxial BFO thin films onto $SrTiO_3$-buffered MgO substrates. They found a band gap value of 2.702 ± 0.007 eV. Li *et al.*[19] investigated the temperature dependence of optical properties of BFO thin films with thickness of about 330 nm prepared on $SrTiO_3$ (111) substrates. It was found that the optical band gap decreases from 2.69 ± 0.01 to 2.65 ± 0.01 eV with increasing temperature.

Despite many studies of the optical properties of BFO thin films, the strain dependence of the optical features and their temperature evolution are less addressed. Moreover, light-induced size changes,[20] photovoltaic effects,[5] and photo-assisted THz emissions[21] have been recently discovered in BFO. These results suggest the possibilities to use BFO in optoelectronic applications. Therefore, to explore the band gap of BFO thin films under various strain states and at high

a)Author to whom correspondence should be addressed. Electronic mail: hliu@ntnu.edu.tw.

temperatures is crucial to determine the threshold photon energy. In this paper, we present a comprehensive strain dependence of ellipsometric spectra in a series of epitaxial BFO thin films. These thin films were grown by pulsed laser deposition as well as MBE on several substrates, namely, $LaAlO_3$ (LAO), $NdGaO_3$ (NGO), LSAT, $SrTiO_3$ (STO), $DyScO_3$ (DSO), and $NdScO_3$ (NSO), having in-plane (IP) average parameters ranging from 3.787 Å for LAO to 4.01 Å for NSO. Such a variety of substrates allows a virtually continuous change of the IP misfit strain $\epsilon_{in} = (a_{av} - a_{bulk})/a_{bulk}\%$ (with a_{av} being the average pseudocubic parameter of BFO) from compressive -4.5% to tensile $+1.2\%$. To avoid structural relaxation, the BFO thickness was set to 30 nm for all samples. Our optical spectra show that the largest value of room-temperature band gap about 3.12 eV is obtained for compressively strained BFO/LAO, and it redshifts to 2.75 eV for tensile strained BFO/NSO thin films. Notably, with increasing temperature, an anomaly observed in band gap that signals antiferromagnetic Nèel temperature is independent of strain and close to its bulk value. These results are in good agreement with those obtained from the first-principles calculations.[6]

The BFO epitaxial thin films with the nominal thickness of about 30 nm were prepared on LAO, NGO, LSAT, STO, DSO, and NSO substrates by pulsed laser deposition and MBE. The crystalline structures of BFO thin films were checked by the x-ray powder diffraction (Rigaku/MiniFlex II). The morphology and microstructure of the samples were examined using scanning electron microscopy (SEM, JEOL 6700 F) and transmission electron microscopy (TEM, JEOL 2100).

Ellipsometric spectra were collected under multiple angles of incidence between 60° and 75° using a Woollam M-2000U rotating compensator multichannel spectroscopic ellipsometer over a spectral range from 0.73 to 6.42 eV. For high temperature measurements, ellipsometer was equipped with a LINKAM heating stage system. Due to the 70° angle of the two stage windows, only a single angle of incidence is possible. The raw ellipsometry data Ψ and Δ are related to the complex Fresnel reflection coefficients for light polarized parallel (R_p) and perpendicular (R_s) to the plane of incidence

$$\tan\Psi e^{i\Delta} = \frac{R_p}{R_s}. \quad (1)$$

To determine the complex dielectric response of BFO thin films, the experimental data were processed using a four-medium optical model consisting of a semi-infinite substrate/-bulk film/surface roughness/air ambient structure. Then the error function σ was minimized in the entire spectral range

$$\sigma^2 = \frac{1}{m}\sum_{i=1}^{m}[(\Delta_{exp} - \Delta_{calc})^2 + (\Psi_{exp} - \Psi_{calc})^2], \quad (2)$$

where Δ_{calc}, Ψ_{calc} and Δ_{exp}, Ψ_{exp} are, respectively, the calculated and experimental ellipsometric data and m is the number of points in the spectrum. The Lorentz approximation was used to fit the spectral dependence of Ψ and Δ and calculate the dielectric function.

Figure 1 displays the room-temperature x-ray powder diffraction profiles of BFO thin films grown on different substrates. All the reflections can be indexed and inferred

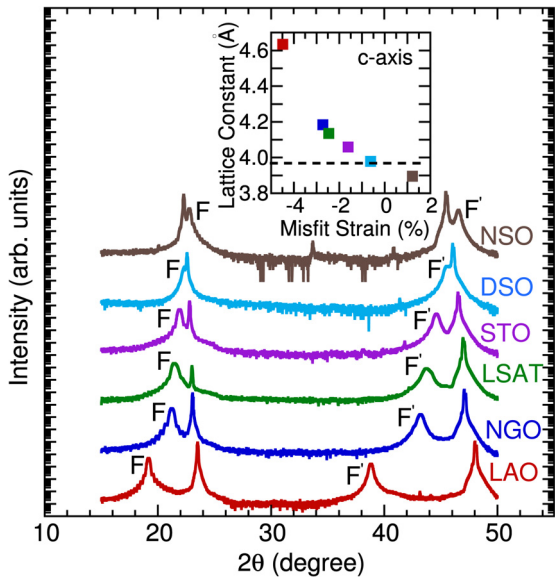

FIG. 1. The x-ray diffraction patterns of BFO thin films grown on different substrates. F and F' represent the (001) and (002) diffraction peaks of BFO thin films. Inset shows the out-of-plane c parameter as a function of the in-plane strain of BFO thin films grown on LAO, NGO, LSAT, STO, DSO, and NSO substrates. Dotted line denotes the value of c-axis lattice constant of bulk BFO.

that BFO thin films grow single phase and epitaxially along the $[001]_C$ direction on all substrates. BFO thin film is tetragonal-like phase on a LAO substrate, rhombohedral phase on NGO, LSAT, STO, and DSO substrates, and orthorhombic phase on a NSO substrate.[22,23] From the Rietveld refinement, we determined the lattice constants of the samples under investigation. The out-of-plane c parameter as a function of IP misfit is shown in the inset of Figure 1. It clearly follows a linear dependence, indicating an elastic deformation of the BFO unit. Thus, using this series of substrates, a large variation of IP strain values has been achieved, from compressive -4.5% to tensile $+1.2\%$.

Figure 2(a) shows the room-temperature real ϵ_1 and imaginary ϵ_2 parts of the dielectric function of BFO thin films on LAO, LSAT, and NSO substrates. In all cases, the dispersive response in ϵ_1 with an overall positive value is an indication of the semiconducting behavior.[24] Optical transitions can be identified in the spectra by resonance and antiresonance features that appear at the same energy in ϵ_2 and ϵ_1, respectively. Notably, the spectrum ϵ_2 of BFO/LAO thin film is dominated by two optical transitions, which are blue shifted and also broadened compared with those of BFO/LSAT and BFO/NSO.

To illustrate the detailed changes of the optical spectra with different substrates, we fit these data using a classical Lorentzian model for the complex dielectric function[25]

$$\epsilon(\omega) = \sum_{j=1}^{N}\frac{\omega_{pj}^2}{\omega_j^2 - \omega^2 - i\omega\gamma_j} + \epsilon_\infty, \quad (3)$$

where ω_j, γ_j, and ω_{pj} are the frequency, damping, and oscillator strength of the jth Lorentzian contribution, and ϵ_∞ is the high frequency limit of $\epsilon(\omega)$ which includes interband transitions at frequencies above the measured range. The absorption coefficient is simply $\alpha(\omega) = \frac{2\omega}{c}$

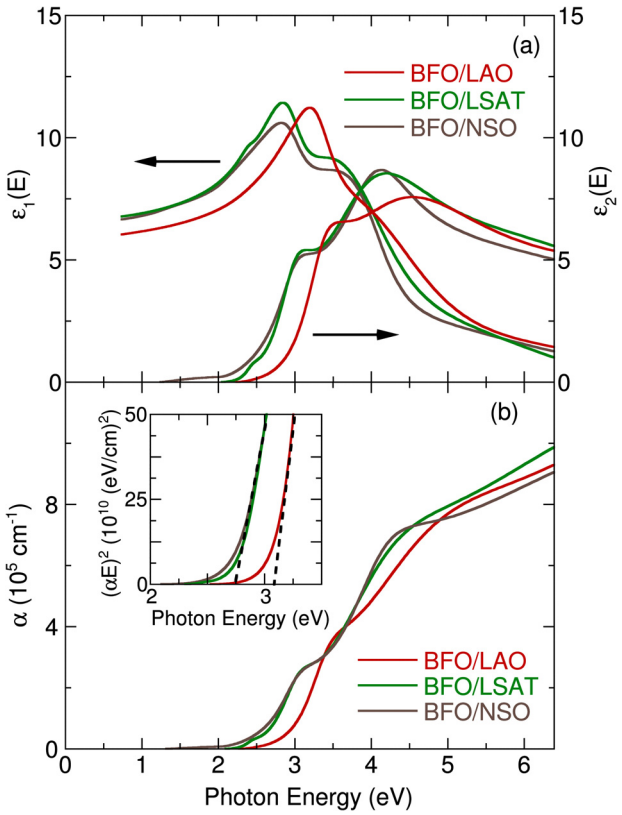

FIG. 2. (a) Room temperature dielectric function spectra of BFO/LAO, BFO/LSAT, and BFO/NSO thin films. (b) Optical absorption coefficient of BFO/LAO, BFO/LSAT, and BFO/NSO thin films at 300 K. In the inset, we show the direct band gap analysis of BFO/LAO, BFO/LSAT, and BFO/NSO thin films.

$\sqrt{\frac{1}{2}[\sqrt{(\epsilon_1(\omega)^2+\epsilon_2(\omega)^2)}-\epsilon_1(\omega)]}$. Figure 2(b) displays the optical absorption spectra of three thin films. We notice that the absorption of BFO/LAO thin film gradually increases and shows two features centered at about 3.5 eV and 5.0 eV that are assigned as minority channel dipole-allowed charge transfer excitations.[13,17] The absorption spectra are overall red shifts by ~0.5 eV and narrowered in BFO/LAST and BFO/NSO thin films.

In a normal solid, one expects that the absorption coefficient, $\alpha(E)$, consists of contributions from both the direct and indirect band gap transitions[26] and is given by

$$\alpha(E) = \frac{A}{E}(E - E_{g,\mathrm{dir}})^{0.5} + \frac{B}{E}(E - E_{g,\mathrm{ind}} \mp E_{\mathrm{ph}})^2, \quad (4)$$

where $E_{g,\mathrm{dir}}$ and $E_{g,\mathrm{ind}}$ are the magnitudes of direct and indirect gaps, respectively, E_{ph} is the emitted (absorbed) phonon energy, and A and B are constants. This model, while assuming a simple band shape, allows for extraction of the direct energy gap by plotting $(\alpha \cdot E)^2$ as a function of photon energy. Linear extrapolation of $(\alpha \cdot E)^2$ to zero in BFO/LAO thin film yields a gap of 3.12 ± 0.05 eV, as shown in the inset of Fig. 2(b). Plotting $(\alpha \cdot E)^{0.5}$ as a function of photon energy led to an unsatisfactory fit, with no evidence for emitted/absorbed phonons. Plots of $(\alpha \cdot E)^2$ versus energy place the band gap in BFO/NGO, BFO/LSAT, BFO/STO, BFO/DSO, and BFO/NSO thin films at $\sim 2.82 \pm 0.05$ eV, 2.82 ± 0.05 eV, 2.82 ± 0.05 eV, 2.81 ± 0.05 eV, and 2.75 ± 0.05 eV, respectively. This strain-dependent evolution of the band gap is mainly due to the lattice expansion effects of the a-b plane in BFO thin films.

Figure 3 shows the temperature dependence of the gap. With increasing temperature, the gap softens for all six samples. The band gap narrowing coefficient can be obtained by the formula $\beta = dE_g/dT$. BFO/LAO thin film has the highest value of the coefficient of about -3.1×10^{-4} eV/K at 298 K. Interestingly, its gap shows anomalies at about 380 K and 640 K. 380 K corresponds to structural transformation between different tetragonal-like phases observed in BFO/LAO thin films.[27,28] 640 K is the Nèel temperature observed in bulk BFO. This result is in good agreement with the previous optical transmittance measurements.[13] In principle, the observed redshift value of the band gap energy with increasing temperature in semiconductors can be described using the Bose-Einstein model[29]

$$E_g(T) = E_g(0) - \frac{2a_B}{[\exp(\Theta_B/T) - 1]}, \quad (5)$$

where $E_g(0)$ is the band gap energy at 0 K, a_B represents the strength of the electron-phonon interactions, and Θ_B is the characteristic temperature parameter representing the effective phonon energy on the temperature scale. In this model, the electron-phonon interactions are responsible for the shrinkage in the band gap with the temperature. Our fitting curves are shown in Fig. 3 with a_B and Θ_B values in a range of 50–70 meV and 200–300 K, respectively. These values are in agreement with the previous results observed in BFO/STO thin films.[19] As is evident from Fig. 3, the Bose-Einstein model reproduces the overall temperature dependence of the band gap in all BFO thin films fairly well. However, it does not

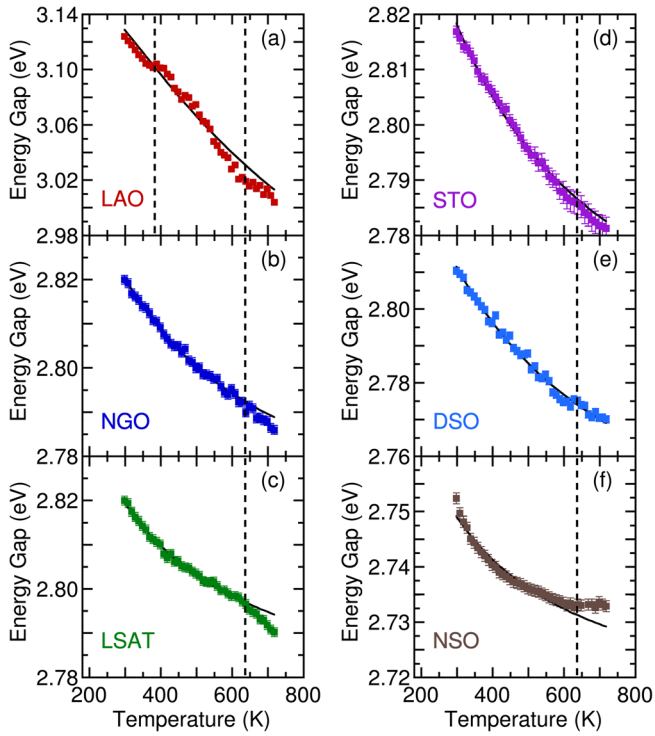

FIG. 3. Energy gap as a function of temperature for all six BFO thin films. The thin solid lines are results of the fitting using the Bose-Einstein model. Vertical dashed lines denote transition temperatures.

capture the discontinuous redshift of the band gap near 380 K and 640 K for BFO/LAO thin films. Notably, the temperature evolution of the band gap spectra for BFO/NGO, BFO/LSAT, BFO/STO, BFO/DSO, and BFO/NSO thin films in Fig. 3 deviates from the theoretical predictions above 640 K. We calculate the temperature dependence of band gap first derivative, and from this, assemble the strain-dependent trends of deviation from the Bose-Einstein expectation. The deviation temperature for six BFO thin films is 643 ± 5 K. Interestingly, the magnitude of deviation is maximum and changing sign for highly compressive strained BFO/LAO and tensile strained BFO/NSO thin films. It is likely due to a change of structural strain and local symmetry breaking in the high temperature phase. Further details of theoretical investigations are needed to confirm this speculation.

Significantly, the observed band gap anomalies near 640 K for all strained BFO thin films imply that antiferromagnetic Nèel temperature is independent of strain and close to its bulk value. Similar evidence has also been inferred from Mössbauer spectroscopy and neutron diffraction measurements.[6] More recently, first-principles calculations predict that the antiferromagnetic transition temperature hardly varies but the ferroelectric Cuire temperature is strongly reduced with strain in BFO thin films.[6] Finally, of particular interest is the deviation of the band gap across T_N from the Bose-Einstein theory. We attribute this observed phenomena mainly due to a complex charge-spin interaction. The deviation for the BFO/LAO and BFO/NSO thin films becomes even larger, indicating the increased coupling between the electronic structure and antiferromagnetic ordering in highly strained BFO.

In summary, we investigated the effects of strain on optical properties in $BiFeO_3$ thin films using spectroscopic ellipsometry. In room temperature optical absorption spectra, we found that compressively strained BFO/LAO thin film has the largest band gap of about 3.12 eV. It redshifts to 2.75 eV for tensile strained BFO/NSO thin films. With increasing temperature, the band gap behaves anomalously above the 640 K antiferromagnetic transition temperature for all strained BFO thin films. These results are in good agreement with the first-principles calculations, which predict the antiferromagnetic Nèel temperature of BFO thin films is independent of strain and close to its bulk value. Most importantly, the antiferromagnetic ordering remains intact, in spite of strain-induced changes of electronic structure, suggesting a complex nature of charge-spin coupling in multiferroic BFO thin films.

We thank financial support from the National Science Council of Republic of China under Grant No. NSC 101-2112-M-003-003.

[1]H. Schmid, Ferroelectrics **162**, 317 (1994).
[2]N. A. Hill, J. Phys. Chem. B **104**, 6694 (2000).
[3]W. Eerenstein, N. D. Mathur, and J. F. Scott, Nature (London) **442**, 759 (2006).
[4]G. Catalan and J. F. Scott, Adv. Mater. **21**, 2463 (2009).
[5]T. Choi, S. Lee, Y. J. Choi, V. Kiryukhin, and S.-W. Cheong, Science **324**, 63 (2009).
[6]I. C. Infante, S. Lisenkov, B. Dupé, S. Fusil, E. Jacquest, G. Geneste, S. Petit, A. Courtial, J. Juraszek, L. Bellaiche, A. Barthélémy, and B. Dkhil, Phys. Rev. Lett. **105**, 057601 (2010).
[7]J. R. Teague, R. Gerson, and W. J. James, Solid State Commun. **8**, 1073 (1970).
[8]J. Li, J. Wang, M. Wuttig, R. Ramesh, N. Wang, B. Ruette, A. P. Pyatakov, A. K. Zvezdin, and D. Viehlanda, Appl. Phys. Lett. **84**, 5261 (2004).
[9]R. R. Das, D. M. Kim, S. H. Baek, C. B. Eom, F. Zavaliche, S. Y. Yang, R. Ramesh, Y. B. Chen, X. Q. Pan, X. Ke, M. S. Rzchowski, and S. K. Streiffer, Appl. Phys. Lett. **88**, 242904 (2006).
[10]D. Ricinschi, K.-Y. Yun, and M. Okuyama, J. Phys.: Condens. Matter **18**, L97 (2006).
[11]C. Ederer and N. A. Spaldin, Phys. Rev. Lett. **95**, 257601 (2005).
[12]P. Ravindran, R. Vidya, A. Kjekshus, H. Fjellvag, and O. Eriksson, Phys. Rev. B **74**, 224412 (2006).
[13]S. R. Basu, L. W. Martin, Y. H. Chu, M. Gajek, R. Ramesh, R. C. Rai, X. Xu, and J. L. Musfeldt, Appl. Phys. Lett. **92**, 091905 (2008).
[14]A. Kumar, R. C. Rai, N. J. Podraza, S. Denev, M. Ramirez, Y.-H. Chu, L. W. Martin, J. Ihlefeld, T. Heeg, J. Schubert, D. G. Schlom, J. Orenstein, R. Ramesh, R. W. Collins, J. L. Musfeldt, and V. Gopalan, Appl. Phys. Lett. **92**, 121915 (2008).
[15]J. F. Ihlefeld, N. J. Podraza, Z. K. Liu, R. C. Rai, X. Xu, T. Heeg, Y. B. Chen, J. Li, R. W. Collins, J. L. Musfeldt, X. Q. Pan, J. Schubert, R. Ramesh, and D. G. Schlom, Appl. Phys. Lett. **92**, 142908 (2008).
[16]S. J. Clark and J. Robertson, Appl. Phys. Lett. **90**, 132903 (2007).
[17]P. Chen, N. J. Podraza, X. S. Xu, A. Melville, E. Vlahos, V. Gopalan, R. Ramesh, D. G. Schlom, and J. L. Musfeldt, Appl. Phys. Lett. **96**, 131907 (2010).
[18]J. Allibe, K. Bougot-Robin, E. Jacquet, I. C. Infante, S. Fusil, C. Carrétéro, J.-L. Reverchon, B. Marcilhac, D. Creté, J.-C. Mage, A. Barthélémy, and M. Bibes, Appl. Phys. Lett. **96**, 182902 (2010).
[19]W. W. Li, J. J. Zhu, J. D. Wu, J. Gan, Z. G. Hu, M. Zhu, and J. H. Chu, Appl. Phys. Lett. **97**, 121102 (2010).
[20]B. Kundys, M. Viret, D. Colson, and D. O. Kundys, Nature Mater. **9**, 803 (2010).
[21]D. S. Rana, I. Kawayama, K. Mavani, K. Takahashi, H. Murakami, and M. Tonouchi, Adv. Mater. **21**, 2881 (2009).
[22]R. J. Zeches, M. D. Rossell, J. X. Zhang, A. J. Hatt, Q. He, C.-H. Yang, A. Kumar, C. H. Wang, A. Melville, C. Adamo, G. Sheng, Y.-H. Chu, J. F. Ihlefe, R. Erni, C. Ederer, V. Gopalan, L. Q. Chen, D. G. Schlom, N. A. Spaldin, L. W. Martin, and R. Ramesh, Science **326**, 977 (2009).
[23]J. C. Yang, Q. He, S. J. Suresha, C. Y. Kuo, C. Y. Peng, R. C. Haislmaier, M. A. Motyka, G. Sheng, C. Adamo, H. J. Lin, Z. Hu, L. Chang, L. H. Tjeng, E. Arenholz, N. J. Podraza, M. Bernhagen, R. Uecker, D. G. Schlom, V. Gopalan, L. Q. Chen, C. T. Chen, R. Ramesh, and Y. H. Chu, Phys. Rev. Lett. **109**, 247606 (2012).
[24]P. Gori, M. Rakel, C. Cober, W. Richter, N. Esser, A. Hoffmann, R. D. Sole, A. Cricenti, and O. Pulci, Phys. Rev. B **81**, 125207 (2010).
[25]F. Wooten, *Optical Properties of Solids* (Academic, New York, 1972).
[26]J. I. Pankove, *Optical Processes in Semiconductors* (Dover, New York, 1971).
[27]J. Kreisel, P. Jadhav, O. Chaix-Pluchery, M. Varela, N. Dix, F. Sánchez, and J. Fontcuberta, J. Phys.: Condens. Matter **23**, 342202 (2011).
[28]K.-Y. Choi, S. H. Do, P. Lemmens, D. Wulferding, C. S. Woo, J. H. Lee, K. Chu, and C.-H. Yang, Phys. Rev. B **84**, 132408 (2011).
[29]L. Vina, S. Logothetidis, and M. Cardona, Phys. Rev. B **30**, 1979 (1984).